Role of Divalency in the High-Affinity Binding of Anticardiolipin Antibody−β_2-Glycoprotein I Complexes to Lipid Membranes

George M. Willems,*,‡ Marie P. Janssen,‡ Maurice M. A. L. Pelsers,‡ Paul Comfurius,‡ Monica Galli,§ Robert F. A. Zwaal,‡ and Edouard M. Bevers‡

Cardiovascular Research Institute Maastricht, University of Limburg, Maastricht, The Netherlands, and Department of Hematology, Ospedale Riuniti, Bergamo, Italy

Received March 18, 1996; Revised Manuscript Received July 8, 1996⊗

ABSTRACT: β_2-Glycoprotein I (β_2GPI) is an essential cofactor for the binding to lipids of anticardiolipin antibodies (ACA), isolated from patients with anti-phospholipid syndrome. We used ellipsometry to study the binding of β_2GPI and the β_2GPI-mediated binding of ACA to planar membranes composed of phosphatidylcholine (PC) and 5−20 mol % phosphatidylserine (PS). No binding of β_2GPI was observed to neutral (PC) membranes. Maximal binding of β_2GPI was 3.2−3.6 pmol·cm^{-2}. Affinity decreased strongly with decreasing PS content; increasing the NaCl and $CaCl_2$ concentrations also led to a decrease in affinity. At physiologic conditions (10 mol % PS, 120 mM NaCl, and 3 mM $CaCl_2$), a K_d of 14 μM was observed. Binding constants were insensitive to the chemical composition of the negatively charged phospholipid headgroup. ACA (1.25−10 μg·mL^{-1}) caused a 30−40-fold enhancement of β_2GPI binding to PS/PC membranes (20 mol % PS), resulting in the binding of about 2 pmol·cm^{-2} divalent ACA−(β_2GPI)$_2$ complexes at 100 nM β_2GPI. In the absence of β_2GPI, binding of ACA was negligible. Ad- and desorption kinetics of ACA−β_2GPI complexes indicate that the initial monovalent association of ACA to membrane-bound β_2GPI is rapidly followed by formation of divalent ACA−(β_2GPI)$_2$ complexes. Experiments with monovalent Fab[1] fragments of ACA showed no appreciable effect on the β_2GPI binding to lipid, substantiating the notion that divalent interactions are essential for the high-affinity binding of ACA−β_2GPI. The anticoagulant effect of ACA is rationalized by the observation that binding of ACA−β_2GPI complexes to the PSPC membrane severely restricts the adsorption of blood coagulation factor Xa.

β_2-Glycoprotein I (β_2GPI)[1] is a plasma protein circulating both as a free protein and associated to lipoproteins. This protein, also referred to as apolipoprotein H, was described for the first time in 1961 by Schultze et al. (Schultze et al., 1961). The protein consists of 345 amino acid residues, including a 19 amino acid N-terminal signal peptide, and is highly enriched in proline residues (Kato & Enjyoji, 1991; Lozier et al., 1984; Matsuura et al., 1991; Mehdi et al., 1991; Steinkasserer et al., 1991). The apparent molecular mass of β_2GPI is estimated at 50 kDa under nonreducing conditions, shifting upward to 70 kDa upon reduction, in agreement with the high number of disulfide bonds. β_2GPI is a single-chain molecule and is highly glycosylated, the variability of which is responsible for the existence of at least five isoforms (Gries et al., 1989; Schousboe, 1982). The amino acid sequence of β_2GPI in human, rat, and bovine appears to be highly conserved; the protein contains 5 internal repeats of 60 amino acid residues, each with 2 internal disulfide bonds, known as short consensus repeats or Sushi domains (Aoyama et al., 1989; Bendixen et al., 1992; Kato & Enjyoji, 1991).

Despite its rather high plasma concentration of 0.15−0.30 mg·mL^{-1} (3−6 μM) (Cleve & Rittner, 1969), little is known about the biological function of β_2GPI; among the proposed functions are modulation of the metabolism of triglyceride-rich lipoproteins (Nakaya et al., 1980), modulation of platelet function (Nimpf et al., 1985a,b; Schousboe, 1980), and inhibition of blood coagulation (Nimpf et al., 1986; Schousboe, 1985), although this latter function has been questioned (Bancsi et al., 1992).

Research on β_2GPI got further impetus by the demonstration that this protein appeared to be the plasma cofactor required for the binding of so-called "anticardiolipin" antibodies (ACA) to an anionic lipid surface (Galli et al., 1990; McNeil et al., 1990). Together with lupus anticoagulants (LA), ACA belong to the family of "antiphospholipid" antibodies whose presence in plasma, in association with clinical manifestations such as arterial and venous thrombosis, recurrent abortion, and thrombocytopenia, defines the "Antiphospholipid Syndrome" (McNeil et al., 1991). It is becoming more appreciated that these antibodies are not directed to phospholipids, but recognize lipid-bound (plasma) proteins; LA was found to be directed to lipid-bound prothrombin (Bevers et al., 1991; Oosting et al., 1993; Permpikul et al., 1994), whereas ACA recognizes lipid-bound β_2GPI (Galli et al., 1990; McNeil et al., 1990; Oosting et al., 1991; Roubey et al., 1992) or even β_2GPI bound to particular plastic surfaces (Matsuura et al., 1994). Evidence

* Address correspondence to this author at the Cardiovascular Research Institute Maastricht, University of Limburg, P.O. Box 616, 6200 MD Maastricht, The Netherlands. Telephone: +31 43 3881651. Fax: +31 43 3670916.

‡ University of Limburg.

§ Ospedale Riuniti.

⊗ Abstract published in *Advance ACS Abstracts,* October 1, 1996.

[1] Abbreviations: ACA, anticardiolipin antibody; β_2GPI, β_2-glycoprotein I; PS, 1,2-dioleoyl-*sn*-glycero-3-phosphatidylserine; PC, 1,2-dioleoyl-*sn*-glycero-3-phosphatidylcholine; PE, 1,2-dioleoyl-*sn*-glycero-3-phosphoethanolamine; PG, 1,2-dioleoyl-*sn*-glycero-3-phosphoglycerol; FXa, blood coagulation factor Xa; Tris, tris(hydroxymethyl)aminomethane; EDTA, ethylenediaminetetraacetic acid.

S0006-2960(96)00657-5 CCC: $12.00

has been presented that the anticoagulant activity of some ACA is mediated via β_2GPI (Galli et al., 1992; Oosting et al., 1991; Roubey et al., 1992). In fact, it was demonstrated that the inhibitory effect of β_2GPI on the conversion of prothrombin to thrombin by the factor Xa−factor Va complex assembled on the lipid surface is strongly enhanced by the presence of ACA (Galli et al., 1992). It is generally assumed that the observed interference with lipid dependent reactions is the consequence of high affinity binding of ACA−β_2GPI complexes to the membrane, thereby restricting the available lipid surface. The precise mechanism of high-affinity binding of ACA to lipid-bound β_2GPI is still unresolved: on the one hand, it has been suggested that ACA binds to a neo-epitope formed on β_2GPI as result of a change in conformation induced by the binding of β_2GPI to the lipid membrane (Matsuura et al., 1994; Wagenknecht & McIntyre, 1993). On the other hand, it was proposed that ACA are low-affinity antibodies which bind to β_2GPI on lipid membranes through a divalent interaction promoted by the enhanced surface density of antigen (Roubey et al., 1995).

The interaction of β_2GPI with negatively charged phospholipids has been demonstrated in several studies (Kertesz et al., 1995; Nakaya et al., 1980; Polz & Kostner, 1979; Schousboe, 1979), but quantitative data on the binding parameters are scarce and regard membranes containing 50−100 mol % negatively charged lipids (Hagihara et al., 1995; Wurm, 1984). In this report, we describe a quantitative study on the interaction of β_2GPI with membranes, composed of lipid mixtures which are more physiological relevant. We used highly purified β_2GPI to characterize its binding to well-defined planar bilayers by means of ellipsometry. In addition, we studied the β_2GPI-mediated binding of ACA to lipid membranes and analyzed adsorption and desorption kinetics in order to elucidate the mechanism of ACA−β_2GPI−lipid interaction.

METHODS

Materials. Bovine serum albumin (BSA, essentially fatty acid free) and cardiolipin (CL) from bovine heart were from Sigma (St. Louis, MO). 1,2-Dioleoyl-*sn*-glycero-3-phosphocholine (PC), 1,2-dioleoyl-*sn*-glycero-3-L-phosphoserine (PS), 1,2-dioleoyl-*sn*-glycero-3-phosphoethanolamine (PE), and 1,2-dioleoyl-*sn*-glycero-3-phosphoglycerol (PG) were purchased from Avanti Polar Lipids (Alabaster, AL). Silicon slides were obtained from Aurel GmbH (Landsberg, Germany). Bovine factor X was purified and activated with Russell's viper venom (Fujikawa et al., 1972a,b), and factor Xa (FXa) was quantitated as described before (Smith, 1973). All other chemicals used were of analytical grade.

SDS−PAGE. SDS−PAGE was performed in 10−15% gradient gels on a Phast system from Pharmacia (Uppsala, Sweden).

Purification of β_2GPI. Human β_2GPI was purified according to previously described methods (Wurm, 1984), with minor modifications. Briefly, perchloric acid (70%) was added to outdated pooled plasma to a final concentration of 1.2% and stirred for 30 min at 0−4 °C. After removal of the precipitate, the supernatant was adjusted to pH 8.0 by adding saturated Na_2CO_3, followed by extensive dialysis against 20 mM Tris, pH 8.0. This material was applied to a QAE column, and proteins were eluted using a gradient from 0 to 350 mM NaCl. β_2GPI-containing fractions, as detected by SDS−PAGE and silver staining, were pooled, dialyzed against 20 mM Tris, pH 8.0, and applied to a heparin affinity column. Bound proteins were eluted using a gradient from 0 to 1.0 M NaCl. Finally, the β_2GPI preparation was further purified by FPLC over Mono-Q, which removed traces of IgG present in the preparation. (Using a less steep gradient, this last step also allowed separation of the various isoforms of β_2GPI.) The final β_2GPI preparation contained a homogeneous band at 50 kDa as shown by unreduced SDS−PAGE and silver staining.

Isolation of ACA and Preparation of Fab1 Fragments. Since we intended to perform a thorough kinetic analysis of the interaction between ACA, β_2GPI, and phospholipids, we restricted ourselves to ACA isolated from one patient. The patient, male, age 45, had repeated peripheral thrombosis, but did not fulfill the criteria for the diagnosis of systemic lupus erythematosus; antibodies, isolated via liposomal adsorption from the plasma of this patient, have been part of earlier studies (Galli et al., 1990, 1992). These ACA can be considered to be representative for the group of ACA patients, based on solid phase immunoassays and lipid-dependent coagulation tests. ACA was isolated by adsorption to cardiolipin-containing liposomes and subsequent affinity chromatography over protein A−Sepharose CL-4B (Fine, Uppsala, Sweden) as described earlier (Galli et al., 1990). The final preparation was run over an anti-β_2GPI affinity column, in order to make sure that ACA was free of β_2GPI contamination.

Fab[1] fragments were obtained from purified ACA by digestion with papain: 1 mL of purified ACA (4.9 mg) was incubated in Tris-buffered saline (TBS) for 4 h with 98 μg of papain (Sigma) at 37 °C. The reaction was stopped by addition of 10 mM iodoacetamide followed by dialysis against TBS. The reaction mixture was subsequently separated by HPLC using a TSK 3000 SW column (Pharmacia). Residual contaminating Fc fragments were finally removed by affinity chromatography over protein A−Sepharose. The final Fab[1] preparation showed a homogeneous band at 50 kDa by unreduced, and 25 kDa by reduced, SDS−PAGE and silver staining.

Phospholipids and Preparation of Lipid Bilayers. Phospholipid concentrations were determined by phosphorus analysis (Böttcher et al., 1962). Planar bilayers were deposited on silicon slides as described previously (Giesen et al., 1991): briefly, the slides were thoroughly cleaned, treated with chromic sulfuric acid, and extensively rinsed with water before use. Small unilamellar vesicles were prepared from lipid mixtures containing variable (5−20 mol %) amounts of PS, PG, PE, or CL complemented with PC. A planar bilayer was deposited on the slide by immersion for 5 min in a stirred suspension of small unilamellar lipid vesicles (30 μM) in Tris buffer (50 mM Tris, 120 mM NaCl, and 3 mM $CaCl_2$, pH 7.5).

Ellipsometric Determination of Protein Adsorption to Lipid Bilayers. Measurement of protein adsorption to planar bilayers is based on the change in reflection coefficients due to the adsorption of very thin (0.1−10 nm) films. Such changes result in an alteration of the polarization state of reflected light, which can accurately be measured using an ellipsometer (Azzam & Bashara, 1977). The instrument and data analysis have been described earlier (Corsel et al., 1985; Cuypers et al., 1983). For measurement on silicon slides and an angle of incidence of 68°, the adsorbed protein mass

($\mu g \cdot cm^{-2}$) is proportional to the change (degrees) in the polarizer reading [$P(t) - P_o$], due to the protein adsorption: $\Gamma(t) = 0.085[P(t) - P_o]$. Binding experiments were performed at ambient temperature (20−22 °C) under continuous stirring in a trapezoidal cuvette in Tris buffer containing 50 mM Tris, 120 mM NaCl, and 0.5 $mg \cdot mL^{-1}$ bovine serum albumin, pH 7.5 (TBSA). In some experiments, different NaCl concentrations were used, and $CaCl_2$ was added to the buffer as indicated in the text and/or figure legends under Results.

Analysis of Equilibrium Binding. The equilibrium binding data were analyzed using the Langmuir model for independent binding sites:

$$\Gamma_{eq} = \Gamma_{max} C/(K_d + C) \quad (1)$$

which relates the amount of protein (Γ_{eq}) bound on the membrane to the protein concentration in solution (C), the dissociation constant K_d, and the maximal protein adsorption (Γ_{max}). The binding parameters K_d and Γ_{max} are estimated by a least-squares fit of this model to experimental data.

Transport-Limited Adsorption and Desorption Kinetics. The intrinsic kinetics of protein binding to macroscopic surfaces often exceed the mass transfer of protein from bulk solution to the surface (Andree et al., 1993; Corsel et al., 1985; Levich, 1962). Thus, the protein in the fluid layer immediately adjacent to the adsorbing surface is depleted, and the local concentration (C_o) is lower than the bulk concentration (C_b). The mass transfer from bulk solution to the surface then is equal to the concentration difference ($C_b - C_o$) times the mass transfer coefficient Δ ($cm \cdot s^{-1}$):

$$(d/dt)\Gamma = \Delta(C_b - C_o) \quad (2)$$

The value of this mass transfer coefficient depends on the flow conditions, e.g. the rotation rate and size of the stirring bar, and the diffusion constant of the protein. For blood coagulation factor Va, a protein with a molecular mass (168 kDa) close to IgG and with a transport-limited initial adsorption rate to PS/PC bilayers (Willems et al., 1993), we found under the experimental conditions used in this study a value $\Delta = 1.0 \times 10^{-3}$ $cm \cdot s^{-1}$.

Kinetics of Adsorption of ACA−β_2GPI Complexes. The model depicted in Scheme 1 was used to analyze the sorption kinetics. The first step is the second-order association reaction of solution phase ACA with membrane-bound β_2GPI:

$$(d/dt)\Gamma_{ACA} = k_{on,1} ACA_o \Gamma_{\beta 2GPI}$$

with Γ_{ACA} the amount of ACA ($pmol \cdot cm^{-2}$) bound to the membrane as ACA−β_2GPI complexes, $k_{on,1}$ the second-order rate constant of association ($M^{-1} \cdot s^{-1}$), ACA_o the concentration (M) of ACA in solution close to the lipid membrane, and $\Gamma_{\beta 2GPI}$ the amount of membrane-bound β_2GPI ($pmol \cdot cm^{-2}$) not associated to ACA. For the rather low ACA concentrations used in this study, adsorption is a slow process with a time scale of 30−150 min (cf. Figure 4). Lipid-bound association reactions generally proceed rapidly because of the high collisional efficiency [$k_{on} \sim 10^{16}$ $mol^{-1} \cdot cm^2 \cdot s^{-1}$ (Giesen et al., 1991)] for two-dimensional reactions in addition to the concentration of protein brought about by binding to the membrane. Even for a value as low as $k_{on,2} = 10^{13}$ $mol^{-1} \cdot cm^2 \cdot s^{-1}$ for the rate constant of association

Scheme 1

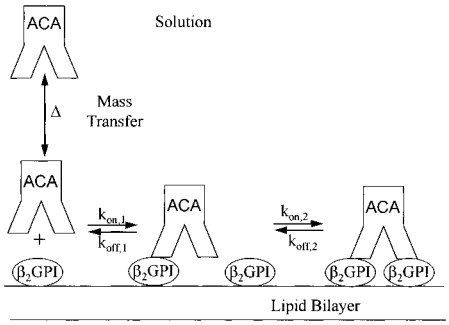

and a surface concentration $\Gamma_{\beta 2GPI} = 10^{-15}$ $mol \cdot cm^{-2}$, the half-time of the secondary divalent binding step is shorter than 1.2 min. Therefore, an instantaneous equilibrium (with respect to the time scale of the adsorption) may be assumed between the mono- and divalently bound ACA. The total adsorption rate is then given by

$$(d/dt)\Gamma_{ACA} = k_{on,1} ACA_o \Gamma_{\beta 2GPI} \quad (3)$$

This equation, which does not account for the transport limitation, predicts an initial adsorption rate linear both with the ACA_o and with the β_2GPI concentration. If, however, $k_{on,1}\Gamma_{\beta 2GPI}$ is of the same order of magnitude or exceeds the mass transfer coefficient Δ, the rapid adsorption of ACA results in depletion of this protein near the adsorbing surface and the ACA concentration near the surface, ACA_o (cf. eq 22), drops appreciably below the bulk concentration. Mass transport must balance the consumption of protein at the surface; combining eqs 2 and 3 allows elimination of ACA_o:

$$\begin{aligned}(d/dt)\Gamma_{ACA} &= \Delta k_{on,1}\Gamma_{\beta 2GPI}/(\Delta + k_{on,1}\Gamma_{\beta 2GPI})ACA_b \\ &= \Delta\Gamma_{\beta 2GPI}/(\Gamma_{\beta 2GPI,ads} + \Gamma_{\beta 2GPI})ACA_b \quad (4)\end{aligned}$$

with $\Gamma_{\beta 2GPI,ads} = \Delta/k_{on,1}$ and ACA_b the concentration of ACA in the bulk solution. Equation 4 predicts a saturable hyperbolic dependence of the adsorption rate on the surface coverage with β_2GPI, $\Gamma_{\beta 2GPI}$, with a half-maximal adsorption rate at a coverage $\Gamma_{\beta 2GPI} = \Gamma_{\beta 2GPI,ads}$. It should be noted that for β_2GPI concentrations well below the dissociation constant, K_d, the amount of β_2GPI bound to the membrane is in good approximation proportional to the solution concentration of β_2GPI, $\Gamma_{\beta 2GPI} = \Gamma_{max,\beta 2GPI}\beta_2GPI/K_{d,\beta 2GPI}$ (cf. eq 1), and the above equation can be rearranged to

$$(d/dt)\Gamma_{ACA} = \Delta[\beta_2GPI/(\beta_2GPI_{o,ads} + \beta_2GPI)]ACA_b \quad (5)$$

with $\beta_2GPI_{o,ads} = (\Delta/k_{on,1})(K_{d,\beta 2GPI}/\Gamma_{max,\beta 2GPI})$ the concentration of β_2GPI that results in a half-maximal adsorption rate.

Kinetics of Desorption of ACA−β_2GPI Complexes. As shown in Scheme 1, it is assumed that desorption of the divalently bound ACA can be neglected, because of the high affinity of the double attachment of both β_2GPI molecules to the lipid. The desorption of ACA from the membrane then proceeds by dissociation of the monovalent ACA−β_2GPI complex:

$$(d/dt)\Gamma_{ACA} = -k_{off,1}\Gamma_{ACA-\beta 2GPI}$$

In the situation that the majority of membrane-associated ACA is present as divalent ACA−$(\beta_2GPI)_2$ complexes ($\Gamma_{ACA} \sim \Gamma_{ACA-(\beta 2GPI)2} \gg \Gamma_{ACA-\beta 2GPI}$), a quasi-steady-state surface

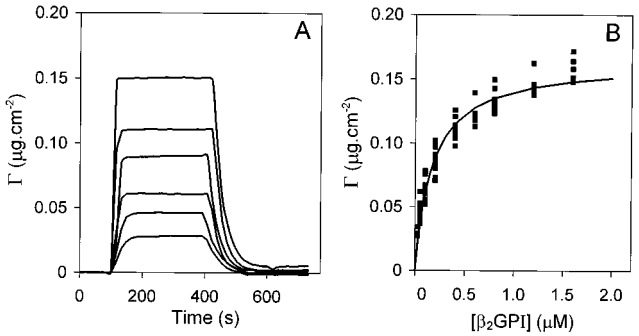

FIGURE 1: Ellipsometric measurement of β_2GPI adsorption to PS/PC bilayers. Adsorption of β_2GPI to PS/PC bilayers containing 20 mol % PS. (A) At $t = 100$ s, β_2GPI (0.025, 0.05, 0.1, 0.2, 0.4, or 1.6 μM) was added to the cuvette, and β_2GPI adsorption to the lipid bilayer was measured by ellipsometry. At 400 s, the protein was depleted from the solution by flushing the cuvette with 30 mL of buffer. (B) Indicated are the equilibrium adsorptions of β_2GPI as a function of the β_2GPI concentration. The solid line represents the best fit of eq 1 to the data. Experiments were performed at room temperature (20−22 °C) in Tris-HCl buffer (pH 7.5, 120 mM NaCl, 50 mM Tris, and 0 mM $CaCl_2$) containing 0.5 mg·mL^{-1} BSA.

concentration of these monovalent ACA−β_2GPI complexes on the lipid membrane is established during desorption, satisfying the relation:

$$(k_{on,2}\Gamma_{\beta 2GPI} + k_{off,1})\Gamma_{ACA-\beta 2GPI} = k_{off,2}\Gamma_{ACA-(\beta 2GPI)2}$$

Elimination of $\Gamma_{ACA-\beta 2GPI}$ from this equation results in

$$(d/dt)\Gamma_{ACA} = -k_{off,2}[k_{off,1}/(k_{on,2}\Gamma_{\beta 2GPI} + k_{off,1})] \times \Gamma_{ACA-(\beta 2GPI)2}$$
$$= -k_{off,2}[\Gamma_{\beta 2GPI,des}/(\Gamma_{\beta 2GPI} + \Gamma_{\beta 2GPI,des})]\Gamma_{ACA} \quad (6)$$

with $\Gamma_{\beta 2GPI,des} = k_{off,1}/k_{on,2}$. Equation 6 therefore predicts that the desorption rate declines, proportional to $1/(\Gamma_{\beta 2GPI} + \Gamma_{\beta 2GPI,des})$, with increasing amounts of bound $\Gamma_{\beta 2GPI}$. $\Gamma_{\beta 2GPI,des} = k_{off,1}/k_{on,2}$ presents the surface coverage of uncomplexed β_2GPI resulting in a half-maximal desorption rate. As in eq 4, $\Gamma_{\beta 2GPI}$ can be replaced by the solution concentration of β_2GPI:

$$(d/dt)\Gamma_{ACA} = -k_{off,2}[\beta_2GPI_{o,des}/(\beta_2GPI_{o,des} + \beta_2GPI)]\Gamma_{ACA} \quad (7)$$

with $\beta_2GPI_{o,des} = (k_{off,1}/k_{on,2})(K_{d,\beta 2GPI}/\Gamma_{max,\beta 2GPI})$ the solution concentration of β_2GPI that corresponds to the half-maximal desorption rate.

RESULTS

Figure 1A shows the adsorption of β_2GPI to PC bilayers containing 20 mol % PS. The initial adsorption rate is high and proportional to the protein concentration. A stable steady-state adsorption is reached within 100 s. At 400 s, the cuvette (4 mL) was flushed with 30 mL of buffer, which effectively depletes the protein from the solution. The resulting desorption of β_2GPI is rapid and virtually complete, showing that β_2GPI adsorption to lipid membranes is reversible. The equilibrium binding isotherm of β_2GPI to PC membranes containing 20 mol % PS is shown in Figure 1B. A least-squares fit of the independent binding sites

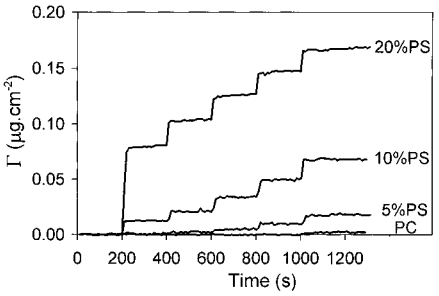

FIGURE 2: Dependence of the binding affinity of β_2GPI on the PS content of the membrane. Adsorption of β_2GPI in response to successive additions of β_2GPI to the cuvette ([β_2GPI] = 0.2, 0.4, 0.8, 1.6, or 3.2 μM) was measured. The curves, from top to bottom, show the binding of β_2GPI to planar PS/PC bilayers containing 20%, 10%, 5%, and 0% PS. Other experimental conditions are as in Figure 1.

Table 1: Binding Parameters of β_2GPI to Planar Phospholipid Membranes[a]

membrane composition	K_d (μM)	Γ_{max} (μg·cm^{-2})
PS/PC (5/95)	26.0	0.17[b]
PS/PC (10/90)	3.7	0.16
PS/PC (20/80)	0.17	0.17
CL/PC (5/95)	2.0	0.17
CL/PC (10/90)	0.12	0.17
PG/PC (20/80)	0.26	0.16

[a] Experiments were performed in Tris-HCl buffer containing 50 mM Tris, 120 mM NaCl, and 0 mM $CaCl_2$. [b] K_d was estimated using a fixed value $\Gamma_{max} = 0.17$ μg·cm^{-2} for the maximal binding.

model of eq 1 resulted in a value of $K_d = 0.17 \pm 0.04$ μM for the dissociation constant and $\Gamma_{max} = 0.165 \pm 0.004$ μg·cm^{-2} for the maximal binding. No obvious deviations between data and the Langmuir model (eq 1) are apparent. Various isoforms of β_2GPI could be obtained by FPLC of the total protein preparation over a Mono-Q column. Binding of the major three of these isoforms of β_2GPI is indistinguishable from that of the total β_2GPI preparation (data not shown), suggesting that the carbohydrate moieties are of minor importance for lipid binding.

Dependence of β_2GPI Binding on the Membrane Composition. Figure 2 shows adsorption of β_2GPI to bilayers of PC supplemented with 0, 5, 10, or 20 mol % PS as a function of time upon stepwise addition of protein to the buffer. Binding to pure PC membranes was found to be negligible. Increasing the PS content results in a strong increase of β_2GPI binding to the membrane. The K_d for a surface containing 5 mol % PS was estimated at 26 μM, which is more than a hundredfold higher than the K_d of 0.17 μM found for membranes with 20 mol % PS. The binding parameters for the different lipid mixtures in Figure 2 are summarized in Table 1. Next we investigated whether the affinity of β_2GPI depends on the chemical composition of the polar headgroup of the negatively-charged membrane component. Binding of β_2GPI to PC membranes containing PG or CL was compared with binding to membranes containing 20 mol % PS. In order to keep the total membrane surface charge comparable to that of a membrane with 20 mol % PS, we used 20 mol % for PG and 10 mol % for CL, the latter having two negative charges per molecule at physiological pH. A dissociation constant of 0.12 ± 0.02 μM and 0.26 ± 0.02 μM was found for bilayers containing CL and PG, respectively, which is only marginally different from that for PS ($K_d = 0.17 \pm 0.04$ μM). In addition, the data in Table 1

Table 2: Effect of NaCl and $CaCl_2$ Concentration on the Binding Affinity of β_2GPI

membrane composition	[NaCl] (mM)	[$CaCl_2$] (mM)	K_d (μM)	Γ_{max} ($\mu g \cdot cm^{-2}$)
PS/PC (20/80)	60	0	0.032	0.18
PS/PC (20/80)	120	0	0.17	0.17
PS/PC (20/80)	120	1	0.63	0.16
PS/PC (20/80)	120	3	3.9	0.18
PS/PC (10/90)	120	0	3.7	0.16
PS/PC (10/90)	120	3	14.0	0.17[a]

[a] K_d was estimated using a fixed value $\Gamma_{max} = 0.17$ $\mu g \cdot cm^{-2}$ for the maximal binding.

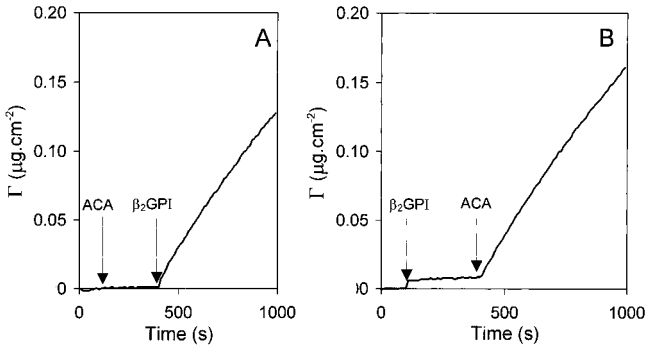

FIGURE 3: Adsorption of anticardiolipin antibodies to lipid membranes requires β_2GPI. Protein adsorption to a planar PS/PC bilayer containing 20 mol % PS after addition of ACA and β_2GPI was measured by ellipsometry. (A) At $t = 100$ s, ACA (5 $\mu g \cdot mL^{-1}$) was added to the cuvette, followed by addition of 100 nM β_2GPI at $t = 400$ s. (B) Similar experiment as shown in panel A, with reversed order of addition of β_2GPI and ACA. Experiments were performed at 20−22 °C in Tris-HCl buffer containing 0.5 $mg \cdot mL^{-1}$ BSA and 3 mM $CaCl_2$.

show that identical values were found for the maximal binding at these different lipid surfaces. In contrast to the findings for PG, CL, and PS, no detectable binding of β_2GPI could be observed for PC bilayers containing 20 or even 40 mol % PE (data not shown).

Dependence of the Affinity of β_2GPI Binding on the Concentration of NaCl and $CaCl_2$. The results obtained so far show that β_2GPI binding depends on the presence of negative charges in the membrane, suggesting that ionic interaction between a positive moiety in the protein with these negative charges governs the binding. This would imply that the affinity is a function of the surface potential of the membrane, which is strongly influenced by the concentration of monovalent and divalent ions in the buffer. Table 2 shows that this indeed is the case. A relatively high affinity for membranes containing 20% PS is observed at low ionic strength (NaCl = 60 mM, $CaCl_2 = 0$ mM), with a dissociation constant ($K_d = 0.032$ μM) 5-fold lower than the $K_d = 0.17$ μM found at 120 mM NaCl. Addition of divalent calcium ions to the buffer at 120 mM NaCl strongly decreased the affinity, resulting in K_d values of 0.63 μM at 1 mM $CaCl_2$ and 3.9 μM at 3 mM $CaCl_2$ and 120 mM NaCl. Similar effects of NaCl and $CaCl_2$ concentrations were found for bilayers containing 10% PS.

Binding of ACA to Membrane-Associated β_2GPI. Figure 3A shows that ACA (5 $\mu g \cdot mL^{-1}$) binding to membranes containing 20 mol % PS is negligible ($<1.5 \times 10^{-3}$ $\mu g \cdot cm^{-2}$). Only after addition of β_2GPI (100 nM) a significant adsorption of protein is observed. Figure 3B shows that under identical conditions (120 mM NaCl and 3 mM $CaCl_2$) 100 nM β_2GPI alone results in a very small, though measurable, protein adsorption (0.005 $\mu g \cdot cm^{-2}$), completed within 40 s. Subsequent addition of 5 $\mu g \cdot mL^{-1}$ ACA initiates an additional protein adsorption comparable to the adsorption shown in Figure 3A. Apparently the adsorption process is insensitive to the order of addition of ACA and β_2GPI. For clarity, Figure 3 only displays the initial phase of the adsorption. In Figure 4, the protein adsorption following addition of varying amounts of ACA (1.25, 2.5, 5, 10 $\mu g \cdot mL^{-1}$) at $t = 100$ s and a fixed amount of β_2GPI (100 nM) at $t = 400$ s was followed up to 3 h. The binding of ACA is apparently a slow process, and for the lower ACA concentrations, the adsorption did not reach equilibrium even after 3 h. A good fit to these data was obtained using the empirical expression $\Gamma(t) = \Gamma_{eq}(1 - e^{-kt})$ which allows estimation of the equilibrium binding Γ_{eq}. A fit of the Langmuir model for independent binding sites (eq 1) to these Γ_{eq} as function of the ACA concentration resulted in a value $\Gamma_{max} = 0.50$ $\mu g \cdot cm^{-2}$ for the maximal binding and a value $K_d = 0.46$ $\mu g \cdot mL^{-1}$ for the concentration ACA resulting in half-maximal equilibrium binding.

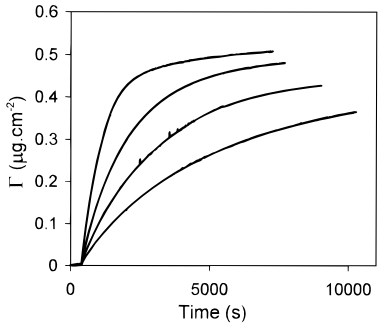

FIGURE 4: Dependence of ACA−β_2GPI adsorption on ACA concentration. (A) Adsorption of ACA−β_2GPI complexes to planar PS/PC bilayers containing 20% PS in the presence of 100 nM β_2GPI and 3 mM $CaCl_2$. ACA concentrations were 1.25, 2.5, 5, or 10 $\mu g \cdot mL^{-1}$ (bottom to top). β_2GPI was added at $t = 100$s followed by addition of ACA at 400 s.

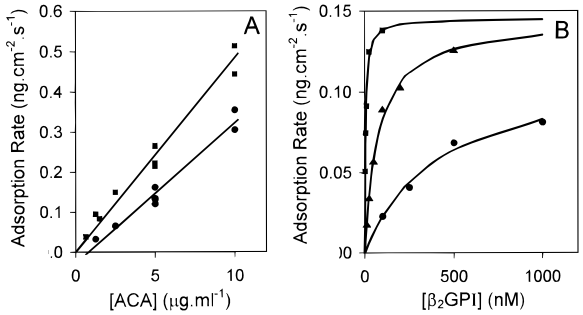

FIGURE 5: Kinetics of ACA− β_2GPI binding. (A) The initial adsorption rate (■) and the adsorption rate at half-maximal surface coverage (●) are presented as a function of the ACA concentration. The β_2GPI concentration was 100 nM. (B) Indicated are the initial adsorption rates as a function of the β_2GPI concentration in the presence of a fixed ACA concentration (1.25 $\mu g \cdot mL^{-1}$): (■) 20% PS in the absence of $CaCl_2$; (▲) 20% PS at 3 mM $CaCl_2$; (●) 10% PS at 3 mM $CaCl_2$. The solid lines represent the best fit of eq 5, $V = V_{max}\beta_2GPI/(\beta_2GPI_{o,ads} + \beta_2GPI)$, to these data.

Kinetics of Adsorption of ACA−β_2GPI Complexes. Experiments as shown in Figure 4 allow estimation of the initial adsorption rate by a least-squares fit of a (second-order) polynomial to the data obtained between 200 and 600 s after addition of protein. Figure 5A, upper line, shows the initial adsorption rate of ACA−β_2GPI complexes as a function of

Table 3: Effect of the β_2GPI Concentration on the Initial Adsorption Rate of ACA−β_2GPI Complexes to Planar Phospholipid Membranes[a]

experimental conditions		V_{max}	$\beta_2GPI_{o,ads}$	$\Gamma_{\beta 2GPI}$
PS/PC	$[CaCl_2]$ (mM)	(ng·cm^{-2}·s^{-1})	(μM)	(pmol·cm^{-2})
20/80	0	0.15	0.005	0.10
20/80	3	0.15	0.075	0.07
10/90	0	0.14	0.12	0.11
10/90	3	0.12	0.42	0.10

[a] The parameters V_{max} and $\beta_2GPI_{o,ads}$ were estimated by a least-squares fit of the formula $V = V_{max}\beta_2GPI/(\beta_2GPI_{o,ads} + \beta_2GPI)$, cf. eq 5, to the initial adsorption rates presented in Figure 5B. $\Gamma_{\beta 2GPI}$ is the amount of β_2GPI bound to the membrane at the half-maximal adsorption rate, calculated using the binding parameters from Tables 1 and 2.

the ACA concentration at a fixed β_2GPI concentration (100 nM). The data clearly show a linear relation between the adsorption rate and the ACA concentration in the range studied (0.63−10 μg·mL^{-1}). The adsorption rates at half-maximal surface coverage ($\Gamma = 0.25$ μg·cm^{-2}), also shown in Figure 5A, again show a linear dependence on the ACA concentration and are consistently lower than the initial adsorption rates. It should be noted that these experiments were performed at a β_2GPI concentration which in the absence of ACA results in only 3% of maximal binding of β_2GPI.

Next we investigated the dependence of the adsorption kinetics on the amount of β_2GPI bound to the membrane. For various concentrations of β_2GPI, and a fixed ACA concentration of 1.25 μg·mL^{-1}, experiments as indicated in Figure 3A were performed, and the initial adsorption rate was determined. In order to vary the amount of bound β_2GPI independently from the solution concentration, these experiments were performed on membranes containing 10 and 20% PS and both in the presence (3 mM) and in the absence of $CaCl_2$ in the buffer. Figure 5B shows that under all conditions the adsorption rate can be saturated at increasing concentrations of β_2GPI. Table 3 shows that in all situations the maximal adsorption rate V_{max} has a similar value (0.12−0.15 ng·cm^{-2}·s^{-1}). In contrast, the β_2GPI concentration, $\beta_2GPI_{o,ads}$, required to attain the half-maximal adsorption rate shows a large variation: from 5 nM for 20% PS in the absence of calcium to 420 nM for 10% PS in the presence of 3 mM $CaCl_2$. The β_2GPI concentration in solution is in equilibrium with uncomplexed β_2GPI bound to the lipid bilayer, and Table 3 shows that this 100-fold difference in β_2GPI concentrations is required to bind similar amounts (0.07−0.11 pmol·cm^{-2}; i.e., 2−3% of maximal binding) of β_2GPI to the membrane. These data demonstrate that membrane-bound β_2GPI regulates the binding of ACA, whereas the ACA−β_2GPI interaction in solution apparently has no influence on the adsorption kinetics of ACA. The value of the second-order association constant calculated from the estimated values of $\beta_2GPI_{o,ads}$, using eq 5 and a value $\Delta = 10^{-3}$ cm·s^{-1} for the transfer coefficient, amounts to $k_{on,1} = (0.9\ -1.4) \times 10^7$ M^{-1}·s^{-1}. Although the ACA preparation was obtained from patient plasma through adsorption to CL-containing liposomes followed by protein A−Sepharose affinity chromatography, the presence of nonspecific IgG in the preparation cannot be excluded. Measurement of V_{max} allows estimation of the concentration of anti-β_2GPI IgG in the ACA preparation (ACA_{true}): according to eq 5, V_{max} equals ΔACA_{true} and using a value $\Delta = 10^{-3}$ cm·s^{-1} for the mass transfer coefficient, it is calculated that a value $V_{max} = 0.12-0.15$ ng·cm^{-2}·s^{-1} at an ACA concentration of 1.25 μg·mL^{-1} corresponds to a value $ACA_{true} = 0.12-0.15$ μg·mL^{-1}. Thus, about 10% of our ACA preparation can be considered specific anti-β_2GPI IgG.

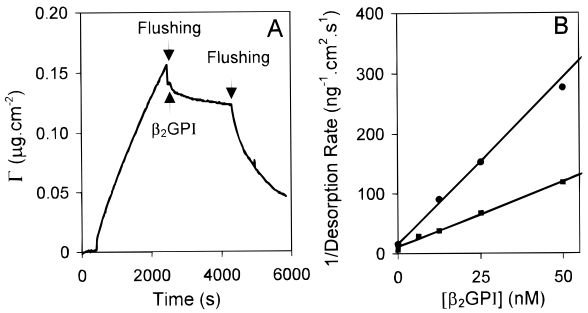

FIGURE 6: Desorption kinetics of lipid-bound ACA−β_2GPI complexes depending on the buffer concentration of β_2GPI. (A) Adsorption of 1.25 μg·mL^{-1} ACA and 100 nM β_2GPI to a planar PS/PC bilayer containing 20% PS at 3 mM $CaCl_2$. The adsorption is interrupted (at $t \sim 2500$ s) by flushing the cuvette with 30 mL of buffer, which resulted in a rapid desorption of protein, immediately followed by addition of 25 nM β_2GPI to the cuvette, causing a marked reduction of the desorption rate. Finally (at $t =$ 4300 s) the cuvette again was flushed with 30 mL of buffer, depleting β_2GPI from the solution which resulted in a steep increase of the desorption rate. (B) Experiments as shown in the left panel were performed in order to obtain the desorption rate as a function of the β_2GPI concentration. Shown is a reciprocal plot of the desorption rate as a function of the β_2GPI concentration at two surface coverages: (■) $\Gamma = 0.3$ μg·cm^{-2}; (●) $\Gamma = 0.1$ μg·cm^{-2}. The solid straight lines represent the best fit to eq 7, $V = V_{max}\beta_2GPI_{o,des}/(\beta_2GPI_{o,des} + \beta_2GPI)$, to these data.

Kinetics of Desorption of ACA−β_2GPI Complexes. Next we studied the kinetics of desorption of ACA−β_2GPI complexes in experiments as shown in Figure 6A. The adsorption of ACA−β_2GPI complexes to a PS/PC bilayer containing 20% PS is interrupted by depletion of β_2GPI and ACA from the solution by flushing the cuvette with 30 mL of buffer. This depletion initiates the desorption of protein from the bilayer. In order to study the influence of the β_2GPI concentration on the desorption rate, β_2GPI (25 nM) is added, and the desorption is followed for 1000−2000 s. Finally, the β_2GPI is again depleted from solution by flushing the cuvette with 30 mL of buffer. Figure 6A shows that the desorption of ACA−β_2GPI complexes proceeds much slower with β_2GPI present in solution than in the absence of β_2GPI. Using experiments as shown in Figure 6A, we measured the desorption rate as a function of the β_2GPI concentration for two ranges of surface coverage (0.08−0.12 and 0.27−0.33 μg·cm^{-2}). Figure 6B shows the reciprocal plot of the measured desorption rates as a function of the β_2GPI concentration. It is clear that the desorption rate steeply decreases with increasing β_2GPI concentrations. This observation is incompatible with monovalent binding of ACA−β_2GPI complexes as in this situation the dissociation rate is unaffected by the presence of β_2GPI in solution or bound to the lipid bilayer. The present results show that desorption of ACA−β_2GPI complexes involves a stage that is sensitive to β_2GPI, presumably the redistribution of lipid-bound ACA between mono- and divalently bound complexes. In addition, eq 7, derived for the dissociation kinetics of divalently bound ACA−β_2GPI complexes, allows a good fit to these data. The estimated values of the parameters V_{max} and $\beta_2GPI_{o,des}$, in Table 4, show that the desorption rate is proportional to the amount of ACA−β_2GPI complexes bound to the membrane and that the desorption rate is half-maximal

Table 4: Effect of the β_2GPI Concentration on the Initial Desorption Rate of ACA−β_2GPI Complexes Bound to Planar PS/PC Membranes[a]

surface coverage (μg·cm^{-2})	V_{max} (ng·cm^{-2}·s^{-1})	$\beta_2GPI_{o,des}$ (μM)
0.1	0.06	0.003
0.3	0.15	0.002

[a] The parameters V_{max} and $\beta_2GPI_{o,des}$ were estimated by a least-squares fit of the formula $V = V_{max}\beta_2GPI/(\beta_2GPI_{o,des} + \beta_2GPI)$, cf. eq 7, to the initial desorption rates presented in Figure 6B.

at a β_2GPI concentration $\beta_2GPI_{o,des} = 2-3$ nM. Even without β_2GPI in solution, the desorption rate is low, corresponding to a first-order rate constant of $k_{off} = 0.5 \times 10^{-3}$ s^{-1}, whereas at 100 nM β_2GPI k_{off} is decreased to 1.7×10^{-5} s^{-1}. Similar experiments performed at 10% PS and 3 mM $CaCl_2$ resulted in values of $k_{off} = 10^{-3}$ s^{-1} and $\beta_2GPI_{o,des} = 20$ nM. The experiments of Figures 3−6 clearly indicate that ACA binds to β_2GPI on the membrane and that the ACA−β_2GPI complexes are predominantly bound as divalent ACA−(β_2GPI)$_2$ complexes. The kinetics of ad- and desorption are fully described by the parameters $k_{on,1} = 1.4 \times 10^7$ M^{-1}·s^{-1}, $\Gamma_{\beta 2GPI,des} = k_{off,1}/k_{on,2} = (2-3) \times 10^{-15}$ mol·cm^{-2}, and $k_{off,2} = 0.5 \times 10^{-3}$ s^{-1}, estimated from these experiments. These are, however, insufficient for a full identification of the adsorption model in Scheme 1, and one additional parameter, e.g., $K_{d,1} = k_{off,1}/k_{on,1}$, is needed.

Monovalent ACA−β_2GPI Interaction. Therefore, we investigated the ACA−β_2GPI interaction of solution phase β_2GPI to ACA immobilized on silicon in the absence of lipid. Adsorption of ACA resulted after about 60 min in an irreversible binding of 2.9 pmol·cm^{-2} IgG. After removal of nonbound ACA from the solution by flushing with 50 mL of buffer, BSA (5 mg·mL^{-1}) was added in order to block aspecific protein binding. The concentration-dependent binding of solution phase β_2GPI to the immobilized ACA was measured by ellipsometry. Control experiments with purified nonspecific human IgG instead of ACA revealed a comparable IgG adsorption but no appreciable β_2GPI binding, demonstrating that aspecific binding could be disregarded. Analysis of the concentration-dependent binding of β_2GPI (0.05−1 μM), using eq 1, resulted in estimates of $\Gamma_{max} = 0.90$ pmol·cm^{-2} and $K_d = 66$ nM for the maximal binding and the dissociation constant, respectively. Assuming identical affinity for ACA to lipid-bound β_2GPI, i.e., $K_{d,1} = k_{off,1}/k_{on,1} = 66$ nM, a full identification of the parameters of Scheme 1 is obtained: $k_{on,1} = 1.4 \times 10^7$ M^{-1}·s^{-1}, $k_{off,1} = 0.9$ s^{-1}, $k_{on,2} = 0.4 \times 10^{15}$ mol^{-1}·cm^{-2}·s^{-1}, and $k_{off,2} = 0.5 \times 10^{-3}$ s^{-1}. Noteworthy is the high affinity of the divalent ACA−(β_2GPI)$_2$ complex with a dissociation constant $K_{d,2} = 1.2 \times 10^{-18}$ mol·cm^{-2}. These data indicate that monovalent ACA binding is weak and that the observed binding results from the high affinity of the divalent interaction of ACA with membrane-associated β_2GPI. This notion was tested in binding experiments of monovalent Fab[1] fragments of ACA to lipid-bound β_2GPI. Figure 7 clearly demonstrates that the adsorption of Fab[1] (5 μg·mL^{-1}) is more than 20-fold lower than the adsorption of ACA at a concentration of 0.5 μg·mL^{-1}. The limited quantity of available Fab[1] did not allow estimation of the dissociation constant of Fab[1] fragments to lipid-bound β_2GPI (which, taking into account the 10% specific activity of the ACA preparation and a K_d of

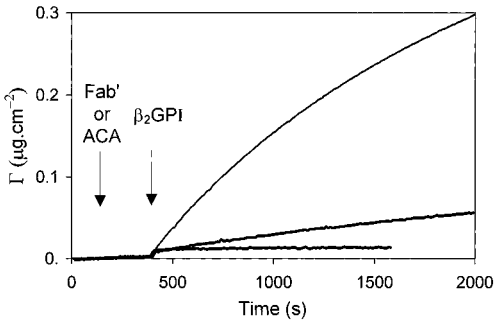

FIGURE 7: Adsorption of Fab[1] fragments of ACA to lipid-bound β_2GPI. Adsorption of 5 μg·mL^{-1} ACA (top curve), 0.5 μg·mL^{-1} ACA (middle curve), and 5 μg·mL^{-1} Fab[1] (bottom curve) in the presence of 100 nM β_2GPI to planar PS/PC bilayers containing 20% PS in the presence of 3 mM $CaCl_2$. Fab[1] or ACA was added at $t = 100$ s and β_2GPI (100 nM) at $t = 400$ s.

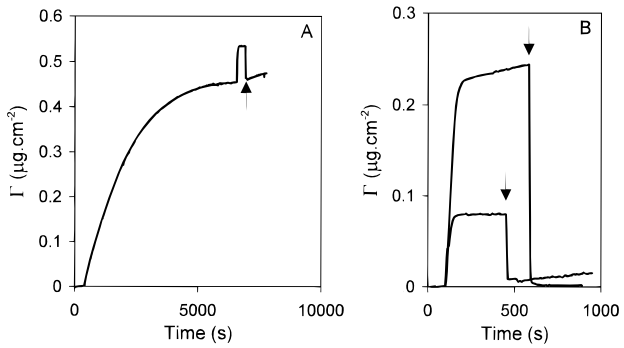

FIGURE 8: Adsorption of ACA−β_2GPI complexes restricts the lipid area available for adsorption of blood coagulation factor Xa. (A) Adsorption of 5 μg·mL^{-1} ACA and 100 nM β_2GPI to planar PS/PC bilayers containing 20% PS in the presence of 3 mM $CaCl_2$. After attainment of equilibrium, 100 nM FXa was added, and additional protein adsorption was observed. Addition of EDTA (6 mM) after the steady state was reached, indicated by an arrow, resulted in complete reversal of the additional FXa adsorption. (B) Indicated are the adsorption of 100 nM FXa to a PS/PC bilayer containing 20% PS (top) in the absence of β_2GPI and ACA and the FXa adsorption from the panel A, corrected for the prior adsorption of the ACA−β_2GPI complexes.

~100 nM, would require concentrations of at least 100 μg·mL^{-1}).

Competition of ACA−β_2GPI Complexes with FXa Binding to the Lipid Membrane. The high-affinity interaction of ACA−β_2GPI complexes with the lipid membrane supports the hypothesis that ACA inhibits membrane-bound reactions of the blood coagulation by restriction of the available lipid surface (Galli et al., 1992). In an attempt to quantitate the effect of ACA−β_2GPI adsorption on FXa binding to the lipid membrane, we performed experiments as shown in Figure 8A. First the adsorption of β_2GPI (100 nM) and ACA (5 μg·mL^{-1}) in the presence of 3 mM $CaCl_2$ was allowed to reach equilibrium; then 100 nM FXa was added to the cuvette, and the additional FXa adsorption was measured. In order to verify that this additional adsorption represents FXa binding, $CaCl_2$ was complexed by addition of EDTA (6 mM), which resulted in a nearly instantaneous protein desorption to the level of the final ACA−β_2GPI adsorption. The slow adsorption, following the FXa desorption, presumably presents a further adsorption of β_2GPI and/or ACA−β_2GPI complexes as a result of the calcium depletion, which causes an increased affinity of β_2GPI (Table 2). Comparison of the adsorption of 100 nM FXa to PS/PC membranes (20% PS) in the presence and absence of preadsorbed ACA−β_2GPI

revealed a 3-fold reduction in adsorption from $\Gamma_{xa} = 0.23 \pm 0.02$ $\mu g \cdot cm^{-2}$ ($n = 3$) to $\Gamma_{xa} = 0.086 \pm 0.06$ $\mu g \cdot cm^{-2}$ ($n = 3$) due to the coverage of the membrane with ACA−β_2GPI complexes ($\Gamma_{ACA-\beta 2GPI} = 0.475 \pm 0.006$ $\mu g \cdot cm^{-2}$; $n = 3$). Preadsorption of ACA in the presence of 500 nM β_2GPI resulted in an even larger reduction of FXa adsorption to $\Gamma_{xa} = 0.062 \pm 0.01$ $\mu g \cdot cm^{-2}$ ($n = 2$). In contrast, partial surface coverage ($\Gamma_{ACA-\beta 2GPI} = 0.21$ $\mu g \cdot cm^{-2}$) with ACA−β_2GPI complexes resulted only in a minor decrease (25%) of the FXa adsorption to $\Gamma_{xa} = 0.174$ $\mu g \cdot cm^{-2}$.

DISCUSSION

Binding of β_2GPI requires incorporation of negative charges in the membrane and is strongly counteracted by increasing the ionic strength or the calcium concentration. These qualitative findings agree with earlier reports (Hagihara et al., 1995; Kertesz et al., 1995; Wurm, 1984). Moreover, the data in Table 1 show that the affinity increases with increasing molar fraction of negatively charged lipid in the mixture but is insensitive to the chemical composition of its headgroup. These results support the notion that binding involves electrostatic interaction between a positively charged sequence in the fifth domain of β_2GPI and negative charges of the lipid polar headgroups (Hunt & Krilis, 1994; Steinkasserer et al., 1991).

For the lipid mixtures studied, 5−20% PS, PG, or CL complemented with PC, the maximal binding of β_2GPI was rather insensitive to the membrane composition and amounted to 0.16−0.18 $\mu g \cdot cm^{-2}$ (3.2−3.6 $pmol \cdot cm^{-2}$), which corresponds to 160 lipid molecules per binding site. For a tightly packed monolayer of spherical molecules with a molecular mass of 50 kDa and a partial specific volume of 0.71 $cm^3 \cdot g^{-1}$ (Fasman, 1976), a maximal binding of 0.36 $\mu g \cdot cm^{-2}$ can be calculated, which is only twice our experimental value, suggesting that the steric hindrance determines maximal binding. For different conditions (large vesicles composed of >50% negatively charged lipids), a stronger effect of the chemical composition of the phospholipid headgroup and of ionic strength on the number of lipid molecules, *n*, per binding site was reported: for CL/PC (50% CL), *n* ranged from $n = 20$ at 10 mM NaCl to $n = 60$ at 300 mM NaCl; *n* was 70 for PS/PC (67% PS) at 10 mM NaCl (Hagihara et al., 1995).

Reported values for the dissociation constant for β_2GPI binding (Hagihara et al., 1995; Wurm, 1984) are low, $K_d = 10^{-8} - 10^{-7}$ M, suggesting a high affinity of β_2GPI for lipid membranes. These values were, however, obtained for membranes containing 50−100% negatively charged lipids, in the absence of calcium and at low (0−10 mM NaCl; $K_d = 10^{-8}$ M) or high (300 mM NaCl; $K_d = 10^{-7}$ M) ionic strength. Similar low values of K_d were found in the present study at 20% PS in the absence of $CaCl_2$ (see Tables 1 and 2). Under physiologically more relevant conditions (120 mM NaCl and 3 mM $CaCl_2$), the dissociation constants for membranes containing 20 and 10% PS were 3.9 and 14 μM, respectively. A plasma concentration of 4 μM β_2GPI will result in less than 25% of maximal binding on 10% PS. Therefore, the function of β_2GPI as a circulating natural anticoagulant seems less likely than previously anticipated; indeed, it has been reported that β_2GPI deficiency does not appear to be associated with clinical symptoms of thrombosis (Bancsi et al., 1992).

This feeble binding of β_2GPI can be enhanced enormously by ACA as shown in Figures 3 and 4. We found a maximal adsorption of ACA−β_2GPI complexes of 0.50 $\mu g \cdot cm^{-2}$, corresponding to 2 $pmol \cdot cm^{-2}$ divalent ACA−(β_2GPI)$_2$ complexes; i.e., 2 $pmol \cdot cm^{-2}$ ACA bound to 4 $pmol \cdot cm^{-2}$ β_2GPI. This latter value is close to the maximal density of binding sites (3.2−3.6 $pmol \cdot cm^{-2}$) found for β_2GPI alone. For planar membranes with 20 mol % PS, in the presence of 3 mM $CaCl_2$ and 100 nM β_2GPI, half-maximal binding required only 0.46 $\mu g \cdot mL^{-1}$ ACA.

In contrast to intact ACA, monovalent Fab[1] fragments caused only minor additional binding (Figure 7). The difference in binding between ACA and Fab[1] is consistent with the model presented in Scheme 1 and reflects the divalent interaction of ACA with lipid-bound β_2GPI. Enhancement of IgG binding due to divalent binding to surface antigens has been demonstrated earlier (Crothers & Metzger, 1972; Greenbury et al., 1965; Hornick & Karuch, 1972; Mason & Williams, 1980; Petrossian, 1993). Divalent interaction generally causes considerable enhancement of the apparent affinity, varying from 30- to 4000-fold. According to the model of Scheme 1, the adsorption rate is described as a bimolecular reaction with a rate proportional to the surface density of the antigen ($\Gamma_{\beta 2GPI}$) and the ACA concentration (ACA_o) in solution near the adsorbing surface. For higher surface densities of β_2GPI, the intrinsic adsorption rate exceeds the rate of mass transfer of ACA from bulk solution to the adsorbing surface, resulting in a lowering of the ACA concentration ACA_o, as accounted for in eq 5. Using this correction, the observed adsorption kinetics (Figure 5) were in excellent agreement with the second-order association kinetics, showing that the initial monovalent association step is rate-limiting and that formation of divalent ACA−(β_2GPI)$_2$ complexes is rapid. The value $k_{on,1} = 1.4 \times 10^7$ $M^{-1} \cdot s^{-1}$ is on the high end of the range $10^4 - 10^7$ $M^{-1} \cdot s^{-1}$ (Hornick & Karuch, 1972; Karlsson et al., 1991; Karush, 1978; Mason & Williams, 1980; Raman et al., 1992) reported for IgG−protein interactions.

The divalent binding of ACA strongly affects the kinetics of desorption: Figure 6 shows a steep decline of the desorption rate with increasing surface densities of β_2GPI at the lipid membrane. This is typical for divalent binding, cf. eq 7, and has been recognized earlier (Mason & Williams, 1980; Ong & Mattes, 1993). For monovalently bound ACA−β_2GPI complexes, the desorption rate is unaffected by the β_2GPI density on the lipid. Only re-adsorption of ACA released from the membrane could affect the desorption kinetics. Using eqs 2−3, it can be calculated that this re-adsorption rate amounts to less than 5% of the desorption rate.

The dissociation constant of the monovalent ACA−β_2-GPI interaction, $K_d = 66$ nM as estimated from the binding of solution phase β_2GPI to ACA immobilized on silicon, is rather high and implies a low affinity for the monovalent interaction of β_2GPI to ACA. Nevertheless, it is about 2 orders lower than the earlier reported value for the ACA−β_2GPI interaction in solution, determined from competition of solution phase β_2GPI with ACA binding to immobilized β_2GPI (Roubey et al., 1995). At present, we have no explanation for this large difference in the estimated affinity, other than differences in patient plasma or in the method of measuring the ACA−β_2GPI interaction. Using the value of 66 nM for the dissociation constant $K_{d,1} = k_{off,1}/k_{on,1}$, we are

able to identify all kinetic parameters of Scheme 1. The value of the association rate constant $k_{on,2} = 0.4 \times 10^{15}$ $mol^{-1}\cdot cm^2\cdot s^{-1}$ approaches the diffusionally limited collision rate, 10^{16} $mol^{-1}\cdot cm^2\cdot s^{-1}$, for membrane-bound reactions (Giesen et al., 1991). In order to appreciate the value $K_{d,2} = 1.2 \times 10^{-18}$ $mol\cdot cm^{-2}$ of the dissociation constant, it is interesting to express this constant in terms of solution phase interactions: 1 $mol\cdot cm^{-2}$ on the lipid surface in a shell of 10 nm thickness corresponds to a concentration of 10^9 M, and therefore the value $K_{d,2} = 1.2 \times 10^{-18}$ $mol\cdot cm^{-2}$ corresponds to 1.2×10^{-9} M, which is nearly 2 orders lower than found for the monovalent ACA−β_2GPI interaction. This comparison, however, is too simplistic as lipid binding of the reactants may cause steric restrictions for complex formation, resulting in changes in affinity. Moreover, for bimolecular reactions, the contribution of the loss in entropy to the change in free energy due to complex formation is less for surface-bound reactants than in solution. It can be calculated, using an ideal gas approximation for the entropy (Adamson, 1973), that this contribution alone would result in the relation $K_{d,surface}(mol\cdot cm^{-2})/K_{d,solution}(M) = 4 \times 10^{-12}$, which is rather close to the ratio found for $K_{d,2}/K_{d,1}$ (2×10^{-11}). Therefore, our results suggest that formation of divalent ACA−β_2GPI complexes at the lipid surface involves only minor steric restrictions. This contrasts with the high steric penalties found for divalent binding of anti-fluorescein IgG to fluorescein haptens incorporated in lipid membranes (Petrossian, 1993).

Our data show that low (3% of maximal binding) surface concentrations of β_2GPI are sufficient to attain maximal binding of ACA−β_2GPI complexes, which seems to contradict the notion that the ACA−β_2GPI interaction requires a high surface density of antigens (Roubey et al., 1995). The latter experiments, however, were performed with β_2GPI attached to a polystyrene surface, causing irreversible binding and immobilization of the protein. As stressed before (Roubey et al., 1995), the immobility of the antigen and the limited flexibility of the IgG molecule will restrict divalent binding to antigens, which are in close proximity. This condition will be extremely rare at low surface densities of antigen. In our experiments, β_2GPI was bound to lipid bilayers with unrestricted lateral mobility of membrane-bound proteins, which obviates this need for high surface coverages.

According to Scheme 1, the surface concentration of β_2-GPI ($\Gamma_{\beta 2GPI}$) regulates the binding of monovalent and divalent ACA−β_2GPI complexes. The ratio of divalent to monovalent complexes equals $\Gamma_{\beta 2GPI}/K_{d,2}$. For $\Gamma_{\beta 2GPI} = 0.1$ $pmol\cdot cm^{-2}$ and a value $K_{d,2} = 10^{-18}$ $mol\cdot cm^{-2}$, this ratio equals 10^5, explaining the huge adsorption of ACA compared to Fab[1] (Figure 7). This regulation of ACA binding by $\Gamma_{\beta 2GPI}$ also presents a problem for the prediction of the ACA−β_2GPI adsorption as function of the ACA and β_2GPI concentrations: competition between adsorbed ACA−β_2GPI complexes and β_2GPI for the available binding sites on the lipid surface cannot be neglected at higher surface coverage, precluding the use of eq 1 to estimate the β_2GPI binding. Such competition for available binding sites is clearly demonstrated for FXa binding in Figure 8: preadsorption of ACA−β_2GPI complexes (90−97% of Γ_{max}) causes a marked decrease (>70%) of FXa binding, but this reduction is much less than the extent of surface coverage by ACA−β_2GPI complexes.

In summary, evidence is presented that the high-affinity binding of ACA−β_2GPI complexes to lipid membranes is a consequence of divalent interactions between the antibody and the membrane-bound β_2GPI. Although the present study does not rule out formation of neo-epitopes on β_2GPI upon binding to lipids, such conformational changes are not required to explain the binding kinetics of ACA−β_2GPI complexes to lipid membranes.

REFERENCES

Adamson, A. W. (1973) *A textbook of physical chemistry*, pp 195−278, Academic Press, New York.

Andree, H. A., Hermens, W. T., & Willems, G. M. (1993) *Colloids Surf., A 78*, 133−144.

Aoyama, Y., Chan, Y. L., & Wool, I. G. (1989) *Nucleic Acids Res. 17*, 6401.

Azzam, R. M. A., & Bashara, N. M. (1977) *Ellipsometry and polarized light*, Elsevier, Amsterdam.

Bancsi, L. F., van der Linden, I. K., & Bertina, R. M. (1992) *Thromb. Haemostasis 67*, 649−653.

Bendixen, E., Halkier, T., Magnusson, S., Sottrup, J.-L., & Kristensen, T. (1992) *Biochemistry 31*, 3611−3617.

Bevers, E. M., Galli, M., Barbui, T., Comfurius, P., & Zwaal, R. F. (1991) *Thromb. Haemostasis 66*, 629−632.

Böttcher, C. J., van Gent, C. M., & Pries, C. (1962) *Anal. Chim. Acta 24*, 203−207.

Cleve, H., & Rittner, C. (1969) *Humangenetik 7*, 93−97.

Corsel, J. W., Willems, G. M., Kop, J. M., Cuypers, P. A., & Hermens, W. T. (1985) *J. Colloid Interface Sci. 111*, 544−554.

Crothers, D. M., & Metzger, H. (1972) *Immunochemistry 9*, 341−357.

Cuypers, P. A., Corsel, J. W., Janssen, M. P., Kop, J. M., Hermens, W. T., & Hemker, H. C. (1983) *J. Biol. Chem 258*, 2426−2431.

Fasman, G. D. (1976) *Handbook of Biochemistry and molecular biology; Proteins*, Vol. II, p 248, CRC Press, Cleveland.

Fujikawa, K., Legaz, M. E., & Davie, E. W. (1972a) *Biochemistry 11*, 4892−4899.

Fujikawa, K., Legaz, M. E., & Davie, E. W. (1972b) *Biochemistry 11*, 4882−4891.

Galli, M., Comfurius, P., Maassen, C., Hemker, H. C., de Baets, M. H., van Breda-Vriesman, P. J., Barbui, T., Zwaal, R. F., & Bevers, E. M. (1990) *Lancet 335*, 1544−1547.

Galli, M., Comfurius, P., Barbui, T., Zwaal, R. F., & Bevers, E. M. (1992) *Thromb. Haemostasis 68*, 297−300.

Giesen, P. L., Willems, G. M., & Hermens, W. T. (1991) *J. Biol. Chem. 266*, 1379−1382.

Greenbury, C. L., Moore, D. H., & Nunn, L. A. (1965) *Immunology 8*, 420−431.

Gries, A., Nimpf, J., Wurm, H., Kostner, G. M., & Kenner, T. (1989) *Biochem. J 260*, 531−534.

Hagihara, Y., Goto, Y., Kato, H., & Yoshimura, T. (1995) *J. Biochem. Tokyo 118*, 129−136.

Hornick, C. L., & Karuch, F. (1972) *Immunochemistry 9*, 325−340.

Hunt, J., & Krilis, S. (1994) *J. Immunol. 152*, 653−659.

Karlsson, R., Michaelsson, A., & Mattsson, L. (1991) *J. Immunol. Methods 145*, 229−240.

Karush, F. (1978) in *Comprehensive immunology; Immunoglobins*, (Litman, G. W., & Good, R. A., Eds.) Vol. 5, pp 85−116, Plenum Press, New York.

Kato, H., & Enjyoji, K. (1991) *Biochemistry 30*, 11687−11694.

Kertesz, Z., Yu, B. B., Steinkasserer, A., Haupt, H., Benham, A., & Sim, R. B. (1995) *Biochem. J. 310*, 315−321.

Levich, V. G. (1962) *Physicochemical hydrodynamics*, Prentice-Hall, Inc., Englewood Cliffs, NJ.

Lozier, J., Takahashi, N., & Putnam, F. W. (1984) *Proc. Natl. Acad. Sci. U.S.A. 81*, 3640−3644.

Mason, D. W., & Williams, A. F. (1980) *Biochem. J. 187*, 1−20.

Matsuura, E., Igarashi, M., Igarashi, Y., Nagae, H., Ichikawa, K., Yasuda, T., & Koike, T. (1991) *Int. Immunol. 3*, 1217−1221.

Matsuura, E., Igarashi, Y., Yasuda, T., Triplett, D. A., & Koike, T. (1994) *J. Exp. Med. 179*, 457−462.

McNeil, H. P., Simpson, R. J., Chesterman, C. N., & Krilis, S. A. (1990) *Proc. Natl. Acad. Sci. U.S.A. 87*, 4120−4124.
McNeil, H. P., Chesterman, C. N., & Krilis, S. A. (1991) *Adv. Immunol. 49*, 193−280.
Mehdi, H., Nunn, M., Steel, D. M., Whitehead, A. S., Perez, M., Walker, L., & Peeples, M. E. (1991) *Gene 108*, 293−298.
Nakaya, Y., Schaefer, E. J., & Brewer, H. B., Jr. (1980) *Biochem. Biophys. Res. Commun. 95*, 1168−1172.
Nimpf, J., Gries, A., Wurm, H., & Kostner, G. M. (1985a) *Thromb. Haemostasis 54*, 824−827.
Nimpf, J., Wurm, H., & Kostner, G. M. (1985b) *Thromb. Haemostasis 54*, 397−401.
Nimpf, J., Bevers, E. M., Bomans, P. H., Till, U., Wurm, H., Kostner, G. M., & Zwaal, R. F. (1986) *Biochim. Biophys. Acta 884*, 142−149.
Ong, G. L., & Mattes, M. J. (1993) *Mol. Immunol. 30*, 1455−1462.
Oosting, J. D., Derksen, R. H., Hackeng, T. M., van Vliet, M., Preissner, K. T., Bouma, B. N., & de Groot, P. G. (1991) *Thromb. Haemostasis 66*, 666−671.
Oosting, J. D., Derksen, R. H., Bobbink, I. W., Hackeng, T. M., Bouma, B. N., & de Groot, P. G. (1993) *Blood 81*, 2618−2625.
Permpikul, P., Rao, L. V., & Rapaport, S. I. (1994) *Blood 83*, 2878−2892.
Petrossian, A. (1993) *Cell Biophys. 23*, 111−137.
Polz, E., & Kostner, G. M. (1979) *Biochem. Biophys. Res. Commun. 90*, 1305−1312.
Raman, C. S., Jemmerson, R., Nall, B. T., & Allen, M. J. (1992) *Biochemistry 31*, 10370−10379.
Roubey, R. A., Pratt, C. W., Buyon, J. P., & Winfield, J. B. (1992) *J. Clin. Invest. 90*, 1100−1104.
Roubey, R. A., Eisenberg, R. A., Harper, M. F., & Winfield, J. B. (1995) *J. Immunol. 154*, 954−960.
Schousboe, I. (1979) *Biochim. Biophys. Acta 579*, 396−408.
Schousboe, I. (1980) *Thromb. Res. 19*, 225−237.
Schousboe, I. (1982) *J. Biochem. Biophys. Methods 6*, 105−114.
Schousboe, I. (1985) *Blood 66*, 1086−1091.
Schultze, H. E., Heide, H., & Haupt, H. (1961) *Naturwissenschaften 48*, 719−724.
Smith, R. L. (1973) *J. Biol. Chem. 248*, 2418−2423.
Steinkasserer, A., Estaller, C., Weiss, E. H., Sim, R. B., & Day, A. J. (1991) *Biochem. J. 277*, 387−391.
Wagenknecht, D. R., & McIntyre, J. A. (1993) *Thromb. Haemostasus 69*, 361−365.
Willems, G. M., Giesen, P. L., & Hermens, W. T. (1993) *Blood 82*, 497−504.
Wurm, H. (1984) *Int. J. Biochem. 16*, 511−515.

BI960657Q